

A Sensorless Initial Rotor Position Estimation Scheme for a Vector Controlled IPMSM Drive

A. Khlaief^(1,2), M. Boussak⁽¹⁾, M. Gossa⁽²⁾

⁽¹⁾ Laboratoire des Sciences de l'Information et des Systèmes (LSIS) UMR CNRS
7296 – Ecole Centrale Marseille (ECM)
Technopole de Château Gombert – 13451 Marseille Cedex 20 – France
mohamed.boussak@centrale-marseille.fr

⁽²⁾ Unité de recherche en Commande, Surveillance et Sûreté de fonctionnement des
Systèmes (C3S) Ecole Supérieure des Sciences et Techniques de Tunis (ESSTT)
5 Avenue Taha Hussein – BP 56, Bab Manara – 1008 Tunis
amor.khlaief@centrale-marseille.fr

Abstract. *Vector field oriented control (VFOC) of permanent magnet synchronous motor (PMSM) drive requires accurate velocity information sensed by a speed or position sensor attached to the rotor. Nowadays, sensorless control is adopted in many industrial applications for reasons of robustness, cost, cabling and reliability. This paper presents a novel sensorless control strategy and initial rotor position estimation for a salient-pole permanent-magnet synchronous motor (IPMSM). Model reference adaptive system (MRAS) technique has been used for speed estimation in sensorless speed control of IPMSM with space vector pulse width modulation (SVPWM). The MRAS technique is simple and it requires less computation time. The stability of the proposed speed estimation technique is achieved through Popov's hyperstability criteria. The initial rotor position is estimated by a suitable sequence of voltage pulses intermittently applied to the stator windings at standstill and the measurement of the peak current values. To illustrate our work, we present experimental results for an IPMSM obtained on a floating point digital signal processor (DSP) TMS320F240 based control system. Experimental results show that the MRAS technique speed estimation provides high performance sensorless control of IPMSM drive.*

Keywords. *Interior permanent magnet synchronous motor (IPMSM), vector field oriented control (VFOC), space vector pulse width modulation (SVPWM), sensorless control, model reference adaptive system (MRAS), initial rotor position detection, digital signal processor (DSP).*

Nomenclature:

$d - q$	Synchronous axis reference frame quantities.
i_α, i_β	Stator α and β axis currents.
i_d, i_q	Stator d and q axis currents.
v_d, v_q	Stator d and q axis voltages.

Φ_d, Φ_q	Stator d and q axis flux linkages.
L_d, L_q	Stator d and q axis inductances.
K_e	Back-EMF coefficient constant.
$\hat{\Phi}_m$	Peak permanent magnet flux.
R_s	Stator resistance.
J	Total rotor inertia.
B	Viscous friction coefficient.
N_p	Number of the pole pairs.
ω_r, θ	Electrical speed and rotor position.
Ω_r	Mechanical rotor speed.
T_e, T_l	Electromagnetic torque and load torque.
p	Laplace variable.
T_s	Sampling period.
T_{sw}	Switching period.
$*$	Reference and estimated value.
$K_{i-\Omega}$ and $K_{p-\Omega}$	Integral and proportional (IP) speed controller.
K_{i-id} and K_{p-id}	Integral and proportional (PI) d -axis current controller.
K_{i-ia} and K_{p-ia}	Integral and proportional (PI) q -axis current controller.
K_{ω_i-est} and K_{ω_p-est}	Integral and proportional (PI) speed observer controller.
T_{sh}	Short time voltage pulses.
T_L	Long time voltage pulses.

1. Introduction

Nowadays, permanent magnet synchronous motor (PMSM) has been widely used in high performance variable speed in many industrial applications, due to its high efficiency, high ratio of torque-to-inertia ratio, high power factor, faster response and rugged construction. The PMSM has increasingly been used in electrical vehicles, aircraft, nuclear power stations, submarines, robotic applications, medical and industrial servo drives. The VFOC is one of the most popular schemes for high performance of PMSM drive control, it is used to control the magnitude of stator and rotor flux and their mutual angle. In order to have a decoupling control between magnetic field and electromagnetic torque, the angle between stator and rotor field should be kept at 90° . Therefore, the d axis reference current is taken as zero ($i_d = 0$). This allows direct control of the flux and torque, in the same manner of an excited DC motor and thus achieves fast dynamic response and high performance. The IPMSM is primarily associated with high performance motor control and is fed by a voltage source inverter (Fig. 1) using SVPWM voltage source inverters (VSI) technique. The presence within electrical drives of rotor speed and position sensors represents a disadvantage under economical aspect because it determines a cost increase, temperature sensitivity and reliability decrease. To overcome these problems, during the last years, there has been considerable interest in sensorless vector control of PMSM drive [1]. A number of sensorless control methods have been proposed in the literature for PMSM [1-16].

Many researchers use the extended Kalman filter EKF technique to estimate the speed and rotor position of the PMSM. Some authors use the dynamic model of the PMSM in $d-q$ axis in the synchronous reference frame fixed to the rotor [2-6] and others use the PMSM model in the $\alpha-\beta$ axis in the stationary reference frame fixed to the stator [7]. It is well known that EKF method is less sensitive to the unknown measurement noise, but requires a long computational time due especially to the huge matrix operations. In [6] the model reference adaptive system (MRAS) was compared with EKF technique and the results confirm that MRAS method is much simpler and faster, but the estimated state of the system is noisier and less precise. Previous methods to estimate the rotor position of permanent magnetic PMSM suffer from the motor parameter variation. In order to overcome this problem, an estimate rotor position of PMSM based on the two sliding mode-based (SMO) have been proposed in [8]. SMO used the estimated speed to correct a stator current observer the correction is based on a sliding mode surface that combines the current error with back EMF estimation. These observers estimate the rotor position and speed from the stator currents and the DC-link voltage measurements. The first observer uses the $\alpha-\beta$ stator reference, while the second observer uses an estimated $d-q$ rotor reference. Other methods are based on high carrier-frequency injection (CFI) technique where the signal is superimposed into the fundamental phase voltages [9-10]. This CFI method gives an information about the rotor position even at very low and zero speed operation due to the electric saliency of the motor. In most cases, the injection signal is a sinusoidal voltage, and the frequency range is 500 Hz. Thus, this may cause acoustic noise, a motor current distortion, torque pulsation and undesirable side effects such as large harmonic losses. The last techniques vector control sensorless PMSM are based on MRAS method [11-19]. In [11], [12], an instantaneous reactive power is used for rotor speed estimation. The advantages of this method are characterized by its independence of stator resistance and are less parameter sensitive of the PMSM. Most observers depend on motor parameters which vary according to temperature. In order to overcome this problem, an on-line parameter identification using adaptive algorithm was proposed in [13]. In [14-17] the authors use the stator currents to estimate the rotor speed and position using MRAS based adaptive strategy applied to non-salient PMSM. Therefore, sensorless methods are widely used to estimate speed and rotor position. Several sensorless techniques are preferred to medium and high speed but are not suitable at standstill. If the PMSM is started without knowing the initial rotor position of the motor, the application of rotating field at an arbitrary position may be accompanied with a temporary reverse rotation of rotor which may lead a starting failure [23-26].

By comparing the methods developed previously in the literature, we can notice that the MRAS technique is one of the best methods to be applied to estimate the rotor speed and position due to its performance in term of consumption less computational time, to its easy implementation in DSP and to its straight forward stability approach. Therefore, in this paper, we propose a MRAS based adaptive speed estimation for sensorless vector control of IPMSM drive with SVPWM. Stability analysis and design of the MRAS estimators have been performed for a IPMSM error model in a synchronous rotating reference frame fixed to the estimated stator $d-q$ axis stator currents. The adaptation mechanism is done by using the error between the measured

and the estimated stator currents. The rotor position can be estimated through a PI controller that controls the speed tuning signal to zero. The stability of the proposed system is guaranteed by the Popov's hyperstability theory. The convergence of the estimated rotor speed and position is guaranteed. At standstill, we propose a new approach to detect the initial rotor position. Short voltage pulses are applied to the stator winding and the initial rotor position is estimated from the measured peak current. The sensorless control approach with initial rotor position estimation of IPMSM drive is applied through in Matlab-Simulink environment and dSpace DS 1103 controller board.

2. Dynamic model of IPMSM

A simplified schematic three phase IPMSM drive fed by voltage source inverter (VSI) controlled by SVPWM technique is shown in Fig. 1. The power circuit of a three-phase VSI is shown in Fig. 1, where v_a, v_b and v_c are the output voltages applied to the star-connected IPMSM windings and V_{DC} is the DC voltage input inverter. T_1 through T_6 are the six IGBT components power module those shape the output, which are controlled by switching signals C_1 to C_6 .

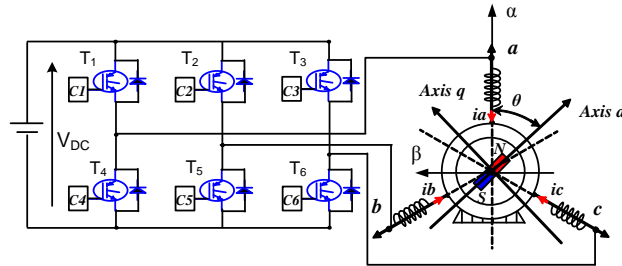


Figure 1. Voltage source inverter fed IPMSM.

Let we develop the state space model of the IPMSM expressed in the synchronous reference frame. The $d - q$ axis stator flux linkages in the synchronous reference frame can be expressed as follows.

$$\Phi_d = L_d i_d + K_e \quad (1)$$

$$\Phi_q = L_q i_q \quad (2)$$

The $d - q$ axis voltage equations in the synchronous reference frame may be expressed as:

$$v_d = R_s i_d + L_d \frac{di_d}{dt} - L_q i_q \omega_r \quad (3)$$

$$v_q = R_s i_q + L_q \frac{di_q}{dt} + (L_d i_d + K_e) \omega_r \quad (4)$$

The electromagnetic torque developed by the motor is:

$$T_e = N_p \left((L_d - L_q) i_d i_q + K_e i_q \right) \quad (5)$$

3. Dead-time compensation

In order to compensate the inverter non-linearity to the ideal reference voltage components in stationary reference frame a compensation signal is added. Voltage drops across power switches in the inverter reduce the terminal voltage seen by motor. At low and high speeds, it is widely known that the dead time causes the fundamental and harmonic distortions of machine currents and voltages. The error in the voltage vector caused by neglecting the forward voltage drop is discussed in [23] is shown that the error voltage vector of the three inverter legs can be represented by:

$$\vec{V}_{fvd} = \frac{2}{3} V_{th} \left[\text{sgn}(i_a) + \alpha * \text{sgn}(i_b) + \alpha^2 * \text{sgn}(i_c) \right] \quad (6)$$

where $\alpha = e^{j2\pi/3}$

From equation (6), it is seen that the voltage error vector only depends on the polarity of the three-phase currents. Hence, for the purpose of compensating the error vector, only the polarities of the three phase currents are needed. There is a time in each switching cycle where both the high and low side switches in the same leg of the inverter are off and the current flow is through diodes. This is known as the dead-time which is inserted into the gate signal of the switch that is to be turned on to avoid direct short circuit across the DC bus voltage source. This dead-time delay causes a change in and distortion of the stator voltage vector applied to the motor. The dead-time error vector between the expected output and actual voltage vector between the expected output and actual voltage vector is given by (7) for different directions of the current vector. This error can be compensated by detecting the polarity of the output current.

$$\vec{V}_{dt} = \frac{2}{3} V_{dead} \left[\text{sgn}(i_a) + \alpha * \text{sgn}(i_b) + \alpha^2 * \text{sgn}(i_c) \right] \quad (7)$$

where

$$V_{dead} = \frac{T_{dead} + T_{on} - T_{off}}{T_{sPWM}} (V_{DC} - V_{sat} + V_f) + \frac{V_{sat} + V_f}{2} \quad (8)$$

where T_{dead} , T_{on} , T_{off} , V_{sat} , V_f are dead time, turn-on time, turn-off time, ON-state voltage drop of the switch and forward voltage drop of the diode respectively. Finally, the stator voltage $\vec{V}_{\alpha,\beta}$ used by the observer is given by:

$$\vec{V}_{\alpha,\beta} = \vec{V}_{ref} - \vec{V}_{dt} \quad (9)$$

The compensation in (9) must be made to the reference voltage vector for more accurate observation.

4. Initial rotor position estimation

In order to achieve correct operation from startup of sensorless IPMSM, the initial rotor position of the motor is required [24-25]. This paper presents a new approach to an improved initial rotor position detection of a IPMSM. With a three-phase inverter legs, we applied three voltage pulses U_1 , U_2 , and U_3 . We used a DSP to generate these pulses to the inputs of power transistors. To apply the voltage pulses we used the configurations of the winding connection presented in Fig. 2.

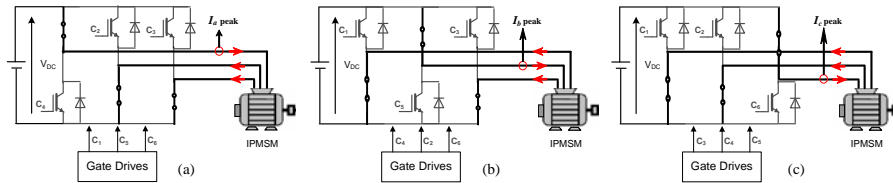


Figure 2. Three possible switching sequences for three-phase IPMSM.

By applying the voltage vector U_1 ($\overline{C1} \overline{C2} \overline{C3}$), the current response of the a phase is dependent on the initial rotor position θ_0 , and can be written as:

$$I_a = I_0 + \Delta I_a = I_0 + \Delta I_0 \cos(2\theta_0) \quad (10)$$

with $I_0 = (1/3)(I_a + I_b + I_c)$: dc current component

ΔI_0 : amplitude of offset value.

In the same way, the expressions of the currents that correspond to the voltage vectors U_2 ($\overline{C1} \overline{C2} \overline{C3}$) and U_3 ($\overline{C1} \overline{C2} \overline{C3}$) are expressed by:

$$\begin{cases} I_b = I_0 + \Delta I_b = I_0 + \Delta I_0 \cos\left(2\theta_0 - \frac{2\pi}{3}\right) \\ I_c = I_0 + \Delta I_c = I_0 + \Delta I_0 \cos\left(2\theta_0 + \frac{2\pi}{3}\right) \end{cases} \quad (11)$$

The expression of the rotor position estimation can be written as:

$$tg(2\theta_0) = -\sqrt{3} \frac{(I_a - I_b)}{2I_a - I_b - I_c} = \sqrt{3} \frac{(I_a - I_b)}{2I_a - I_b - I_c} \quad (12)$$

We can notice that a monotonous function permits to replace the stator currents by their respective difference ΔI_a , ΔI_b , and ΔI_c . Applying the first-order approximation to equation (11), we get the expression of the initial rotor position estimation [24].

$$\theta_0 = \frac{\sqrt{3}}{2} \frac{(\Delta I_a - \Delta I_b)}{(2\Delta I_a - \Delta I_b - \Delta I_c)} \text{ or } \theta_0 = \frac{\sqrt{3}}{2} \frac{(\Delta I_a - \Delta I_b)}{(2\Delta I_a - \Delta I_b - \Delta I_c)} + \pi \quad (13)$$

According to the equation (13), there are two values of rotor position because of two solutions. This problem will also be addressed and a solution is proposed. The proposed method is based on the sign of the peaks and the current differences peaks. If the duration of voltage pulses is low, the total magnet flux not saturates the magnetic circuit. The currents peaks of the stator phases I_a , I_b and I_c can be used to plot the phase current differences ΔI_a , ΔI_b and ΔI_c as function of the rotor position. Fig. 3 shows the experimental results of the peak current differences for each phase.

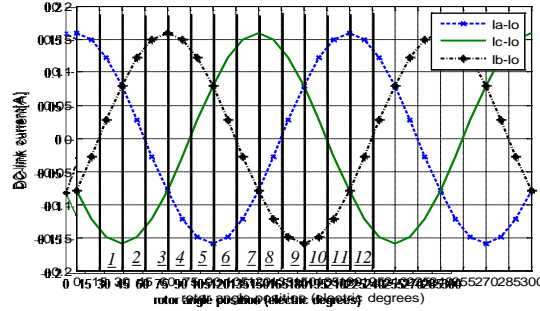


Figure 3. The measured difference of current peaks.

According to the Fig. 3, it is possible to detect the initial rotor position with precision within 15° electric degrees. Its periodicity is two times of electrical angle, therefore, there are two possible values. To remove this ambiguity, we propose a method permitting to make a discrimination of the two values of the initial rotor position. A long time voltage pulse is necessary to distinguish the North pole from the South pole magnet position. This large voltage pulse is necessary to distinguish the North pole from the South pole as will be shown later in this section [26]. This method explores only the magnetic saturation and not the spatial saliency of the IPMSM. The currents peaks imposed into the motor are large enough to change the saturation state of the magnetic circuit. If the magnet flux is in the same direction to the one generated by the current pulse, we get an additive flux and therefore a large peak current. In the opposite case, we obtain a decreasing field. While making a synthesis of this approach to distinguish the North magnetic pole between θ_0 and $\theta_0 + 180^\circ$ electric degrees, we obtain the following table:

Table 1: Discrimination of the initial rotor position look-up table

Voltage pulse	Peak value of the current	Location of the initial position
$U_1(C_1\bar{C}_2\bar{C}_3)$	$I_a > I_b, I_a > I_c$	$-60^\circ < \theta_0 < 60^\circ$
$U_2(\bar{C}_1C_2\bar{C}_3)$	$I_b > I_a, I_b > I_c$	$60^\circ < \theta_0 < 180^\circ$
$U_3(\bar{C}_1\bar{C}_2C_3)$	$I_c > I_b, I_c > I_a$	$180^\circ < \theta_0 < 360^\circ$

The saturation is reached for voltage pulse time duration of $700 \mu\text{s}$, and the current peak is approximately twice the nominal current. Therefore, a high peak current is needed to distinguish the North pole from the South pole. The duration of the voltage vector is $700 \mu\text{s}$, although the constant time of the motor is about 6.8 ms. A high current is needed to distinguish the North pole from the South pole.

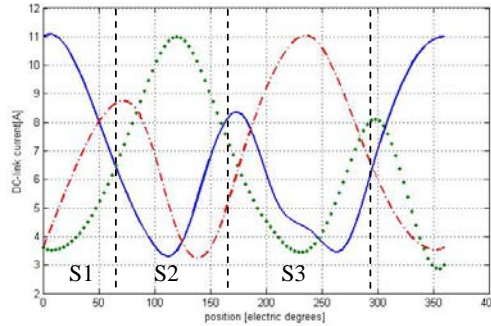


Figure 4. Magnetic pole location.

According to the Fig. 4, we can deduce that the values of the peak current in the saturated condition are in concordance with the Table 1. Indeed, while comparing the peak values of the currents in magnetic saturation, we can overcome the ambiguity on the estimated initial rotor position.

Table 2: Table of initial sector detection.

Initial sector	Initial rotor position (θ_0°)	V_i
Sector1	$\in [0^\circ 60^\circ]$	V_1
Sector2	$\in [60^\circ 120^\circ]$	V_2
Sector3	$\in [120^\circ 180^\circ]$	V_3
Sector4	$\in [180^\circ 240^\circ]$	V_4
Sector5	$\in [240^\circ 300^\circ]$	V_5
Sector6	$\in [300^\circ 360^\circ]$	V_6

In the case of IPMS motors drive fed by VSI controlled by SVPWM technique, the starting from an unknown initial sector may be accompanied by a temporary reverse rotation or may cause a starting failure. Consequently, the knowledge of these inverter states is necessary for sensorless position detection at standstill. Table 2 gives the correspondence between the initial rotor position and the initial sector in the six inverter states.

5. Structure of the proposed MRAS technique

The MRAS estimators are designed to estimate the stator $d-q$ axis currents and the rotor speed. The main idea behind MRAS method is that there is a reference model and an adjustable model where the first one is used to determine the required states and the second one as an adaptive model provides the estimated values of the states. The output of the reference model is compared with an adjustable observer-based model. The error obtained between the reference and adjustable model is given to an adaptation mechanism which adjusts the adaptive model by generating the estimated value of the rotor speed. This strategy allows us to estimate stator currents to converge to the measurement values.

From (3) and (4) the state space $d-q$ axis stator currents of IPMSM designed as reference model is given by:

$$\frac{d}{dt}[X]=[A][X]+[B][U]+[C] \quad (14)$$

$$\text{where } [X]=\begin{bmatrix} i_d \\ i_q \end{bmatrix}, [A]=\begin{bmatrix} -\frac{1}{\tau_d} & \frac{L_q}{L_d}\omega_r \\ -\frac{L_d}{L_q}\omega_r & -\frac{1}{\tau_q} \end{bmatrix}, [B]=\begin{bmatrix} \frac{1}{L_d} & 0 \\ 0 & \frac{1}{L_q} \end{bmatrix}, [U]=\begin{bmatrix} v_d \\ v_q \end{bmatrix}, [C]=\begin{bmatrix} 0 \\ -\frac{K_e}{L_q}\omega_r \end{bmatrix}$$

The state space $d-q$ axis stator currents of IPMSM designed as adjustable model is given by:

$$\frac{d}{dt}[\hat{X}]=[\hat{A}][X]+[B][U]+[\hat{C}] \quad (15)$$

$$\text{where } [\hat{X}]=\begin{bmatrix} \hat{i}_d \\ \hat{i}_q \end{bmatrix}, [\hat{A}]=\begin{bmatrix} -\frac{1}{\tau_d} & \frac{L_q}{L_d}\hat{\omega}_r \\ -\frac{L_d}{L_q}\hat{\omega}_r & -\frac{1}{\tau_q} \end{bmatrix}, [B]=\begin{bmatrix} \frac{1}{L_d} & 0 \\ 0 & \frac{1}{L_q} \end{bmatrix}, [U]=\begin{bmatrix} v_d \\ v_q \end{bmatrix}, [\hat{C}]=\begin{bmatrix} 0 \\ -\frac{K_e}{L_q}\hat{\omega}_r \end{bmatrix}$$

where $L_d, L_q, \tau_d, \tau_q, K_e$ are considered as constant.

After developing adjustable and reference models, the adaptation mechanism will be built for MRAS method. The adaptation mechanism is designed in a way to generate the value of estimated speed used so as to minimize the error between the estimated and reference $d-q$ axis stator currents. By adjusting the estimated rotational speed, the error between the reference and the estimated $d-q$ axis stator currents from (15) is reduced. The error between the estimated and reference $d-q$ axis stator currents are defined as:

$$\varepsilon_d = i_d - \hat{i}_d, \quad \varepsilon_q = i_q - \hat{i}_q \quad (16)$$

The value of the rotor speed error is given as:

$$\Delta\omega_r = \omega_r - \hat{\omega}_r \quad (17)$$

The state currents error component is:

$$\begin{bmatrix} \frac{d\varepsilon_d}{dt} \\ \frac{d\varepsilon_q}{dt} \end{bmatrix} = \begin{bmatrix} -\frac{1}{\tau_d} & \frac{L_q}{L_d}\omega_r \\ -\frac{L_d}{L_q}\omega_r & -\frac{1}{\tau_q} \end{bmatrix} \begin{bmatrix} \varepsilon_d \\ \varepsilon_q \end{bmatrix} + \begin{bmatrix} \frac{L_q}{L_d}i_q \\ -\frac{L_d}{L_q}i_d - \frac{K_e}{L_q} \end{bmatrix} \Delta\omega_r \quad (18)$$

Using equation (18), the state error model of the IPMSM expressed in the $d-q$ synchronous reference frame is given as follow:

$$\frac{d}{dt}[\varepsilon]=[A_\Delta][\varepsilon]+[W] \quad (19)$$

where $[\varepsilon]=[\varepsilon_d \quad \varepsilon_q]^T$ is the error state vector, $[A_\Delta]$ is the state matrix and $[W]$ is the output vector of the feedback block defined as follow:

$$[A_A] = \begin{bmatrix} -\frac{1}{\tau_d} & \frac{L_q}{L_d} \omega_r \\ -\frac{L_q}{L_d} \omega_r & -\frac{1}{\tau_q} \end{bmatrix}, [W] = \begin{bmatrix} \frac{L_q}{L_d} i_q \\ -\frac{L_d}{L_q} i_d - \frac{K_e}{L_q} \end{bmatrix} \Delta \omega_r$$

According to [17], to ensure the hyperstability of the system can be achieved, two criterions must be established. Firstly, the linear time-invariant forward path transfer matrix, $H(p) = (p[I] - [A_A])^{-1}$ must be strictly positive real and secondly, the nonlinear feedback (which includes the adaptation mechanism) must satisfies the following Popov's criterion for stability.

$$\int_0^{t_0} [\varepsilon]^T [W] dt \geq -\gamma^2 \tag{20}$$

where $t_0 \geq 0$, γ is a finite positive real constant, which is independent of t_0

By using the Popov's theory, we obtain: $\lim_{t \rightarrow \infty} [\varepsilon(\infty)]^T = 0$ and therefore, the system of the MRAS speed estimation is asymptotically stable. Finally, from (19), we can conclude that the observed rotor speed satisfies the following adaptation laws:

$$\hat{\omega}_r = \frac{1}{p} A_1 + A_2 \tag{21}$$

where $A_1 = K_1 \left[\frac{L_q}{L_d} i_q \varepsilon_d - \varepsilon_q \left(\frac{L_d}{L_q} i_d + \frac{K_e}{L_q} \right) \right]$; $A_2 = K_2 \left[\frac{L_q}{L_d} i_q \varepsilon_d - \varepsilon_q \left(\frac{L_d}{L_q} i_d + \frac{K_e}{L_q} \right) \right]$, K_1 and

K_2 are the positive adaptation gains.

The speed tuning signal is minimized by PI controller which generates the estimated rotor speed and is fed back to the adaptive model as shown in Fig. 5. The rotor estimated speed is generated from the adaptation mechanism using the error between the estimated and reference currents obtained by the model as follows:

$$\hat{\omega}_r = K_{i\omega_r_est} \int_0^t \left(\frac{L_q}{L_d} i_q \varepsilon_d - \frac{L_d}{L_q} i_d \varepsilon_q - \frac{K_e}{L_q} \varepsilon_q \right) dt + K_{p\omega_r_est} \cdot \left(\frac{L_q}{L_d} i_q \varepsilon_d - \frac{L_d}{L_q} i_d \varepsilon_q - \frac{K_e}{L_q} \varepsilon_q \right) + \hat{\omega}_r(0) \tag{22}$$

where $K_{i\omega_r_est}$ and $K_{p\omega_r_est}$ are the PI speed observer controller and $\hat{\omega}_r(0)$ is the initial estimated speed.

Finally the estimated rotor position is obtained by integrating the estimated rotor speed.

$$\hat{\theta} = \int_0^t \hat{\omega}_r dt + \theta_0 \tag{23}$$

where θ_0 is the initial rotor position estimated by the algorithm described in section 4. The estimating performance of rotor speed is designed only by the PI coefficients.

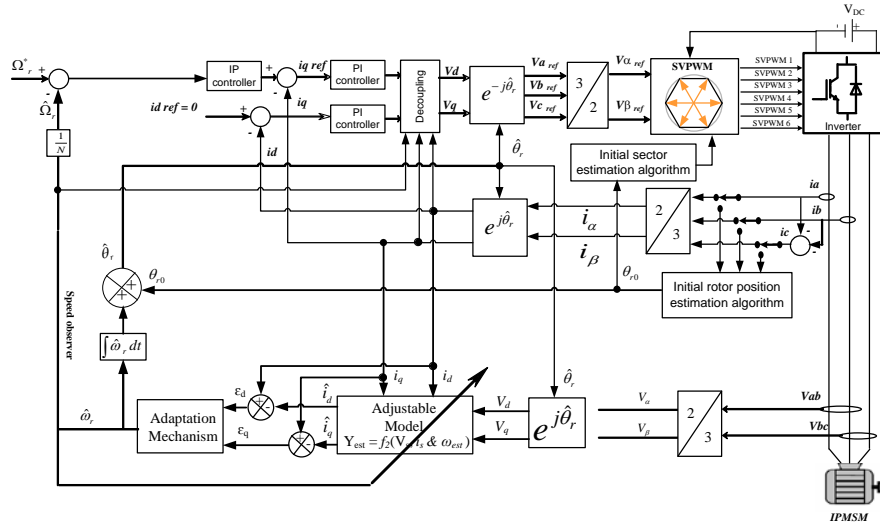


Figure 5. Sensorless VFOC IPMSM drive using MRAS technique.

The proposed SVPWM using MRAS based speed estimation for sensorless field oriented control of IPMSM drive is shown in Fig. 5. From the IPMSM described below, we carried out using Matlab-Simulink to simulate VFOC sensorless speed control taking into account the decoupling stator vector components.

6. Real-time implementation

The experiments presented in this work have been carried out with a DSP board. A DSP is a type of microprocessor that has been designed specially to implement the algorithms required to process signals digitally. These algorithms are characterized by repetitive mathematical computation at high-speed, similar to this application where the mathematically intensive VFOC and SVM algorithms must be run within every 150 μ s sampling period T_s . The system is based on Motorola Power PC604, the DSP subsystem, based on the Texas Instruments TMS320F240 DSP fixed-point processor, the DSP provides 3-phase SVPWM generation making the subsystem useful for drive applications. Two LEMs current sensors (LEM LA 100P) are used to measure the phase current.

7. Experimental results

The model used for SVPWM sensorless VFOC for an IPMSM drive is implemented using dSpace DS1103 and Matlab-Simulink environment. The carrier frequency of SVPWM waveform used in the experimentation is 14 KHz with a dead time of 2 μ s (T_{dead}). In order to verify the effectiveness and the dynamic performances of the proposed sensorless algorithm, many experimental tests have been carried out (Fig. 6 and Fig. 7).

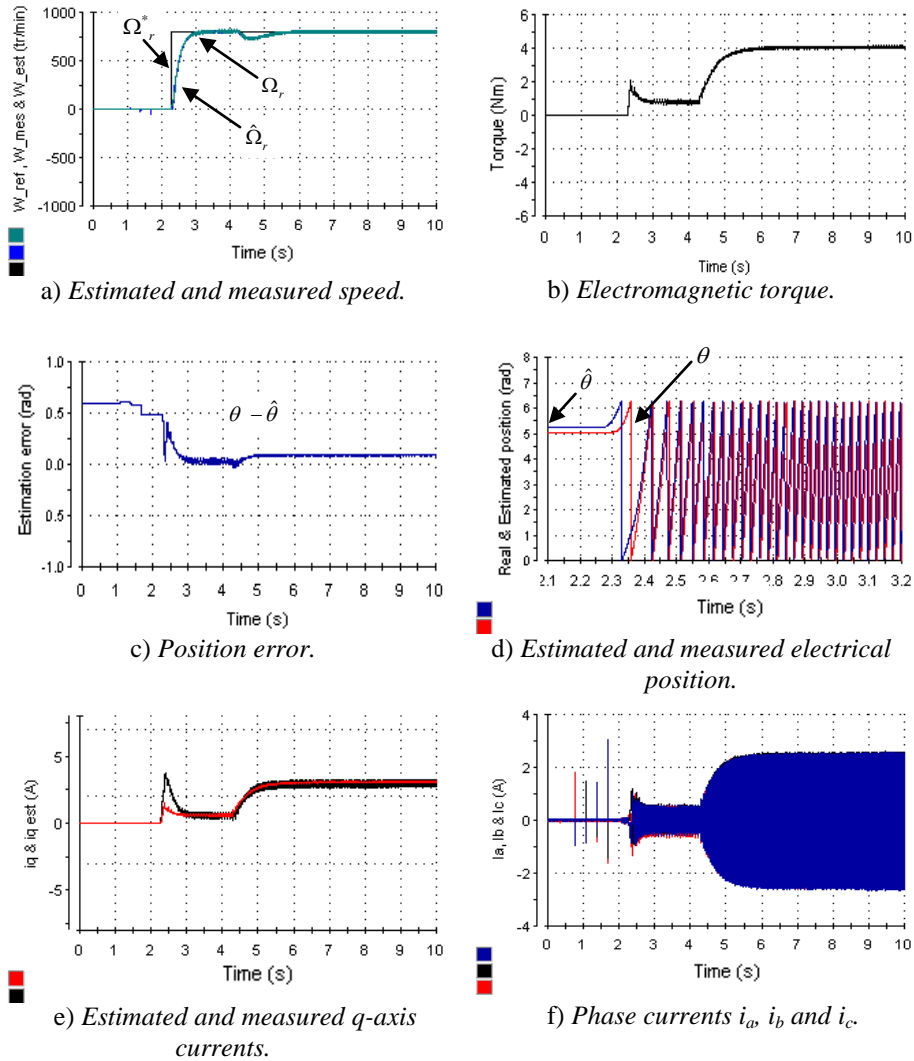
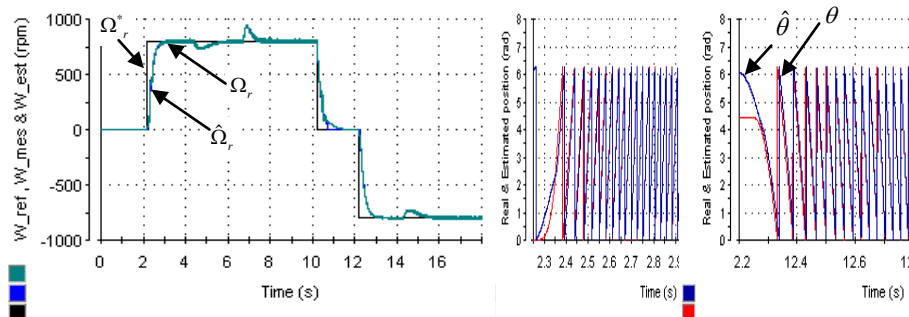


Figure 6. Experimental results with speed reference of 800 rpm under 100% rated load condition.

Fig. 6 illustrates the speed, electromagnetic torque, electrical position and stator currents of the sensorless speed drive at a 800 rpm due to nominal load torque steps. The load was initially applied to the motor and was subsequently removed. We can observe that the estimated position tracks the actual rotor position very well and the estimation error is very small during the transients and steady-state. Hence, the sensorless speed drive is capable of low speed operation with full-load. In linear condition, the signal test must have short time $T_{sh} = 200 \mu s$. The experimental tests show that for $T_L = 700 \mu s$, the saturation is reached and the current peak is approximately twice the nominal current. The standstill algorithm detects the initial

rotor position with peak current after one second. The motor starts rotating with estimated rotor position with MRAS algorithm. During the initial rotor position detection, the four voltage vectors are applied. Fig. 6(a) (before starting) shows the speed responses at standstill when the voltage pulse with short time T_{sh} and with long time T_L is applied to the stator windings of the motor. We can see that the rotor did not move, but it is in a critical position of unstable balance and we note the occurrence of a small vibration on the rotor. Fig. 6(d) shows an example of initial rotor position estimation with the start-up of the motor. After monitoring the peak currents (Fig. 6(f)), the estimated initial rotor position is about 5.58 electrical radians (Fig. 6(d)). According to the experimental results, the estimated position shows good correspondence to the actual rotor position with an average error of a less than electrical angle radians (Fig. 6(c)) which corresponds to about 0.05 electrical angle radians. The motor starts in the desired direction when the speed reference is applied. When $t = 4.2$ s, a load torque is applied and we can observe that the estimated and measured q -axis stator current is directly proportional to the electromagnetic torque (Fig. 6(b)), the results are shown in Fig. 6(e). The result in Figs. 7 shows the performance of the MRAS observer tracking the rotational speed in all speed range. In Fig. 7(a), the performance of the proposed sensorless speed algorithm is again assessed by changing the speed reference from 800 rpm to stand-still and then to -800 rpm. The motor accelerates to 800 rpm and the nominal load torque is applied at time $t = 4$ s, after it is decelerated to zero speed. At time $t = 12$ s, the reference speed is changed from -800 rpm. Finally, the nominal load torque is applied at time $t = 14$ s. The estimated speed follows the actual speed during the reversal and at zero speed operations showing the effectiveness of the proposed sensorless IPMSM drive. Therefore, the performance of a sensorless control algorithm during speed transients and zero speed is verified.



a) Estimated and measured mechanical rotor speed.

b) Zoomed estimated and measured electrical position.

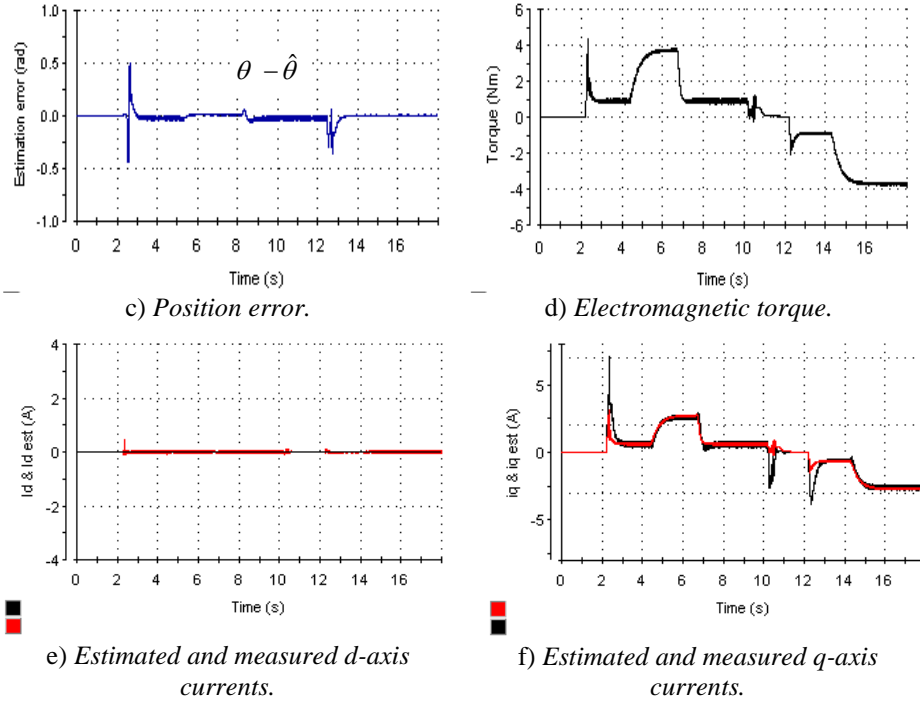


Figure 7. Experimental results with speed reference profile under 100% rated load condition.

These results confirm the choice of the IP speed controller and confirm that there is no overshoot in the step speed response. Fig. 7(b) shows a good agreement between the measured and estimated electrical rotor position and proves the agreement of the proposed method. These results show that MRAS sensorless vector control of IPMSM can accurately estimate the speed and rotor position during the speed reversal and can meet the precision requirements of the system. In Fig. 7(c), the results show the position error under speed changes with nominal load torque condition. The position error using the MRAS method with load condition is not bigger than 0.5 electrical radians, during transients and about 0.08 electrical radians at steady state. Position estimation using MRAS sensorless control is robust under the transient step load torque change and reversal speed. The experimental results presented in Fig. 7(d) show the measured electromagnetic torque. The bandwidth of the speed controller is usually below the bandwidth of the $d-q$ axis stator currents controllers. Fig. 7(e) shows the experimental waveforms of estimated d -axis stator current and measured current step response. We can observe that these currents show a low noise but they are maintained to zero during all the experimental time. Fig. 7(f) shows that the estimated q -axis stator current is tracking the measured one in both directions and varies proportionally with the load torque. The switching ripple is not clearly seen in the stator currents because we have used a low pass filter in the $d-q$ axis currents.

However, we notice that the experimental results show an improved and robust performance in the SVPWM sensorless VFOC algorithm for IPMSM. The experimental results (Fig. 6 and Fig. 7), shows a good agreement and confirms the effectiveness of the proposed rotor speed estimation method.

8. Conclusion

In this paper, a novel sensorless speed control and initial rotor position estimation including magnet polarity for IPMSM has been proposed. The initial rotor position estimation is based on a sequence of voltage pulses and the properties of permanent magnets. By applying a long time voltage pulse to the stator phase winding, we can overcome the ambiguity on the estimation initial rotor position. A sensorless speed control for SVPWM inverter fed IPMSM drive is implemented using MRAS based adaptive speed estimation. The MRAS technique is simple and it uses simplified expressions in the reference and adjustable models with a capability to reduce the mathematical computation time. The proposed sensorless speed control and initial rotor position estimation has been experimentally validated using a dSpace DS1103 with a powerful processor. The experimental results are obtained both in transient step load torque and reversal speed conditions. Moreover, the measured and estimated rotor speeds are accurately tracking their reference during speed transients and stand-still operation. The results clearly demonstrate the good performances and the high dynamic behavior of the proposed IP speed controller. Experimental results have proved the effectiveness of the proposed method based on MRAS technique. In the future work, we intend to estimate online the stator resistance, in order to improve the robustness of the sensorless control.

Appendix

Table 3: Permanent magnet synchronous motor parameters

Parameters		Specification	
R_s	7.2 Ω	Rated power	1.1 kW
L_d	25.025 mH	Rated voltage	400 V
L_q	40.17 mH	Rated current	2.53 A
Φ_{md} (rms)	0.305 Wb	Number of pole pairs	3
K_e	0.5283 V.s.rad ⁻¹	Rated speed	3000 r/min
J	0.0036 Kg.m ²	Rated torque	4 N.m
B	0.0011 Nm.s.rad ⁻¹	DC link voltage	540 V

References

- [1] Singh, B., Singh, B. P., Dwivedi, S. "A review of sensor reduction techniques in permanent magnet synchronous motor drives," *Proc. International Journal of Power and Energy Systems.*, vol. 29, pp. 10–18, 2009.
- [2] Kim, Y. H., Kook, Y. S. "High performance IPMSM drives without rotational position sensors using reduced-order EKF," *Proc. IEEE Trans. Energy. Conversion.*, vol. 14, pp. 868–873, December 1999.
- [3] Bolognani, S., Zigliotto, M., Zordan, M. "Extended-range PMSM sensorless speed

- drive based on stochastic filtering,” *Proc. IEEE Trans. Power. Electron.*, pp. 26, pp. 110–117, January 2001.
- [4] Akin, B. B. “A comparative study on non-linear state estimators applied to sensorless AC drives: MRAS and Kalman filter,” *Proc. IECON, Industrial Electronics Society conference.*, pp. 2148–2153, May 2004.
- [5] Boussak, M. “Implementation and experimental investigation of sensorless speed control with initial rotor position estimation for interior permanent magnet synchronous motor drive,” *Proc. IEEE Trans. Power. Electron.*, vol. 20, pp. 1413–1421, November 2005.
- [6] Bianchi, N., Bolognani, S., Jang, J., Sul, S. “Comparison of PM motor structures and sensorless control techniques for zero-speed rotor position detection,” *Proc. IEEE Trans. Power. Electron.*, vol. 22, pp. 2466–2475, June 2007.
- [7] Hu, J., Liu, J., Eddy, Xu, L. “Eddy current effects on rotor position estimation and magnetic pole identification of PMSM at zero and low speeds,” *Proc. IEEE Trans. Power. Electron.*, vol. 23, pp. 2565–2575, September 2008.
- [8] Andreescu, G. D., Popa, A., and Spilca, A. “Two sliding mode based observers for sensorless control of PMSM drives,” *Proc. Elect. Power Compon. Syst.*, vol. 30, pp. 121–133, February 2002.
- [9] Raca, D., García, P., Reigosa, D. D., Briz, F., Lorenz, R. D. “Carrier-signal selection for sensorless control of PM synchronous machines at zero and very low speeds,” *Proc. IEEE Trans. Ind. Applic.*, vol. 46, pp. 167–178, October 2010.
- [10] Yoo, A., Sul, K. S. “Design of flux observer robust to interior permanent-magnet synchronous motor flux variation,” *Proc. IEEE Trans. Ind. Applic.*, vol. 45, pp. 1670–1677, September 2009.
- [11] Maiti, S., Chakraborty, C., Sengupta, S. “Simulation studies on model reference adaptive controller based speed estimation technique for the vector controlled permanent magnet synchronous motor drive,” *Proc. Simulation Modelling Practice and Theory.*, 17(4):585-596, April 2009.
- [12] Kim, Y. S., Choi, Y. K., Lee, J. H. “Speed sensorless vector control for PMSM based on instantaneous reactive power in the wide-speed region,” *Proc. IEE Electric Power Applications Proceedings.*, vol. 152, pp. 1343–1349, September 2005.
- [13] An, Q., Sun, L. “On-line parameter identification for vector controlled PMSM drives using adaptive algorithm,” *Proc. Vehicle Power and Propulsion conference.*, pp. 1–6, November 2008.
- [14] Liang, Y., Li, Y. “Sensorless control of PM synchronous motors based on MRAS method and initial position estimation,” *Proc. Sixth International on Electrical Machines and Systems conference*, pp. 96–99, November 2003.
- [15] Zhifu, W., Qizhi, T., Chengning, Z. “Speed identification about PMSM with MRAS,” *Proc. Power Electronics and Motion Control Conference.*, pp. 1880–1884, May 2009.
- [16] Sam, K. Y., Kim, S. K., Kwon, Y. A. “MRAS based sensorless control of permanent magnet synchronous motor,” *Proc. SICE conference*, pp. 1632-1637, 2003.
- [17] Kojabadi, H. M., Ghribi, M. “MRAS-based adaptive speed estimator in PMSM drives,” *Proc. of Advanced Motion Control Conference.*, pp. 569–572, May 2006.
- [18] Andreescu, G. D. “Adaptive observer for sensorless control of permanent magnet synchronous motor drives,” *Proc. Elect. Power Compon. Syst.*, vol. 30, pp. 107–119, February 2002.
- [19] Wang, M. S., Kung, Y. S., Hanh, N. T., and Chang, C. M. “Adaptive low-speed control of permanent magnet synchronous motors,” *Proc. Elect. Power Compon. Syst.*, vol. 39, pp. 563–575, March 2011.
- [20] Adamidis, G., Koutsogiannis, Z., and Vagdati, P. “Investigation of the performance of a variable-speed drive using direct torque control with space vector modulation,” *Proc. Elect. Power Compon. Syst.*, vol. 39, pp. 1227–1243, August 2011.

- [21] Wong, K. C., Ho, S. L., and Cheng, K. W. E. "Direct torque control of a doubly-fed induction generator with space vector modulation," *Proc. Elect. Power Compon. Syst.*, vol. 36, pp. 1337–1350, November 2008.
- [22] Sutikno, T., Hwa W. J., Jidin A., and Idris, N. N. R. "A simple approach of space-vector puls width modulation realization based on field programmable gate array," *Proc. Elect. Power Compon. Syst.*, vol. 38, pp. 1546–1557, December 2010.
- [23] S-Y. Kim, W. Lee, M-S. Rho, S-Y. Park. "Effective dead-time compensation using a simple vectorial disturbance estimator in PMSM drives," *Proc. IEEE Trans. Ind. Electron.*, vol. 57, pp. 1609–1614, May 2010.
- [24] Khlaief, A., Boussak, M., Jemli, M., Gossa, M. "Détection de la position initiale du rotor des moteurs synchrones à aimants," *Proc. Journées Tunisiennes d'Electrotechnique et d'Automatique, JTEA'2008*, May 2008.
- [25] Liu, T. H., Hung, C. K., and Chen, D. F. "A matrix converter-fed sensorless PMSM drive system," *Proc. Elect. Power Compon. Syst.*, vol. 33, pp. 877–893, August 2005.
- [26] Rostami, A., Asaei, B. "A novel method for estimating the initial rotor position of PM motors without the position sensor," *Proc. Energy. Convers. Manag.*, vol. 50, pp. 2451–2460, February 2009.
- [27] B. Asaei, A., Rostami. "A novel starting method for BLDC motors without the position sensors," *Proc. Energy. Convers. Manag.*, vol.50, pp. 337–343, February 2009.